AGU PUBLICATIONS

JGR

Journal of Geophysical Research: Solid Earth

RESEARCH ARTICLE

10.1002/2017JB014131

Key Points:
- We develop a theory for slow relaxation and aging in unconsolidated granular earth materials
- The theory attributes the aging process to the slow configurational rearrangement and contact changes of the constituent grains
- We demonstrate good agreement with measurements on simulated fault gouge after the cessation of external disturbances

Correspondence to:
C. K. C. Lieou,
clieou@lanl.gov

Citation:
Lieou, C. K. C., Daub, E. G., Ecke, R. E., & Johnson, P. A. (2017). Slow dynamics and strength recovery in unconsolidated granular earth materials: A mechanistic theory, *Journal of Geophysical Research: Solid Earth*, *122*. https://doi.org/10.1002/2017JB014131

Received 23 FEB 2017
Accepted 3 SEP 2017
Accepted article online 8 SEP 2017

Slow Dynamics and Strength Recovery in Unconsolidated Granular Earth Materials: A Mechanistic Theory

Charles K. C. Lieou[1,2], Eric G. Daub[3], Robert E. Ecke[2,4], and Paul A. Johnson[1,2]

[1]Solid Earth Geophysics Group, Los Alamos National Laboratory, Los Alamos, NM, USA, [2]Center for Nonlinear Studies, Los Alamos National Laboratory, Los Alamos, NM, USA, [3]Center for Earthquake Research and Information, University of Memphis, Memphis, TN, USA, [4]Condensed Matter and Magnet Science Group, Los Alamos National Laboratory, Los Alamos, NM, USA

Abstract Rock materials often display long-time relaxation, commonly termed aging or "slow dynamics," after the cessation of acoustic perturbations. In this paper, we focus on unconsolidated rock materials and propose to explain such nonlinear relaxation through the shear-transformation-zone theory of granular media, adapted for small stresses and strains. The theory attributes the observed relaxation to the slow, irreversible change of positions of constituent grains and posits that the aging process can be described in three stages: fast recovery before some characteristic time associated with the subset of local plastic events or grain rearrangements with a short time scale, log linear recovery of the elastic modulus at intermediate times, and gradual turnover to equilibrium steady state behavior at long times. We demonstrate good agreement with experiments on aging in granular materials such as simulated fault gouge after an external disturbance. These results may provide insights into observed modulus recovery after strong shaking in the near surface region of earthquake zones.

Plain Language Summary This paper presents a theory of slow relaxation and aging in granular earth materials and demonstrates good agreement between the theory and experimental measurements in laboratory fault materials composed of glass beads. Understanding slow relaxation in earth materials helps us gain deeper understanding of the response of the Earth to disturbances such as seismic waves.

1. Introduction

Long-time relaxation, or slow dynamics, is frequently observed in Earth due to strong shaking from earthquakes. For instance, following the *M*6.0 2004 Parkfield earthquake, velocities measured on surface and borehole arrays showed a pronounced decrease in measured velocities characterized by a long recovery spanning over a decade exhibiting log time behavior (e.g., Brenguier et al., 2008; Li et al., 2006; Rubinstein & Beroza, 2005). The affected zone was found to depths of several kilometers (Wu et al., 2016). Such behavior has also been observed elsewhere such as following the 2011 *M*9.0 Tohoku-Oki earthquake on the island of Honshu (Brenguier et al., 2014; Minato et al., 2012; Nakata & Snieder, 2012). These observations are becoming more common and point to induced damage and material healing following a large earthquake.

In more detail, elastic waves of strain amplitudes exceeding about 10^{-6} at ambient pressure and temperature conditions induce nonlinear elastic (and potentially plastic) effects. These include modulus decrease and the slow dynamic recovery. This behavior is due to "damage" at many scales—including grain contact changes as well as deformation associated with existing defects and damage from the length scale of dislocations up to the crack and fracture scale. The modulus decrease is termed "nonlinear fast dynamics" in the literature (e.g., Guyer & Johnson, 2009). After the fast dynamics, the features heal at different rates, culminating in an ensemble behavior generally described by a sequence of exponentials followed by logarithmic time recovery. In short, laboratory studies of both consolidated and unconsolidated materials, including those conducted at room temperature and pressure, suggest that these nonlinear effects can be induced at the contact scale as well as at larger scales where cracks and fractures can be mobilized, leading to a bulk softening behavior that recovers or heals after the wave energy leaves the system (Guyer & Johnson, 2009; Jia et al., 2011; Johnson & Jia, 2005; Johnson & Sutin, 2005; TenCate, 2011; TenCate et al., 2000; van den Wildenberg et al., 2013).

There are a handful of theoretical models for slow dynamics in the physics and rock mechanics literature. For example, Guyer and McCall (Guyer et al., 1995; McCall & Guyer, 1994) introduce hysteretic elastic elements within the Preisach-Mayergoyz (PM) space framework. Scalerandi et al. (2003) attribute material relaxation to the random, thermally activated transitions of mesoscopic elastic finite elements also within the PM space framework. Aleshin and Abeele (2007) attribute the slow relaxation to the mechanics and statistics of internal microcontacts in a similar fashion, noting that the slow increase of the number of contacts during relaxation results in modulus recovery. The "soft ratchet" model of Vakhnenko et al. (2004) proposes a direct relationship between the elastic modulus and a defect density controlled by stress and temperature alone. Lebedev and Ostrovsky (2014) assumes that the strain recovery rate in a relaxation process is controlled by a thermodynamic barrier. Snieder et al. (2016) derive the logarithmic recovery as a superposition of relaxation processes that occur with a generic spectrum of fixed relaxation time. Some of these models (e.g., Guyer et al., 1995; McCall & Guyer, 1994; Scalerandi et al., 2003; Snieder et al., 2016) are purely phenomenological and, in some cases, are purely mathematical exercises. Others (e.g., Aleshin & Abeele, 2007; Lebedev & Ostrovsky, 2014; Vakhnenko et al., 2004) contain more physics, but we attempt to go deeper here. A detailed description of viscoplasticity at the building block level, and the statistical physics of the building blocks, would help us gain deeper insight into the relaxation process in an aggregate material and into the dynamics of earth materials in response to disturbances. This improvement of understanding is precisely the goal of our work: to introduce more physical ingredients that constrain the phenomenology.

In this work we focus on healing at the grain-to-grain scale in the upper crust, as is observed in experiments using unconsolidated grains (Johnson & Jia, 2005). Our model for viscoplasticity and slow recovery in unconsolidated granular media is the shear-transformation-zone (STZ) theory; it is based on the idea that plasticity is attributed to the change of local contacts and rearrangement of grains at loose spots known as STZs and that one can describe the density of these sites using a structural, effective temperature termed the compactivity. When applied to dense granular flow, the STZ theory has been able to describe observations such as the thinning of the shear zone at intermediate shear rates for angular grains (Lieou et al., 2014) and stick-slip instabilities (Lieou et al., 2016, 2015). The STZ theory was originally conceived for plastic deformation in amorphous solids such as metallic glasses (Falk & Langer, 1998, 2011; Langer, 2008), based on an analogous idea that plasticity in amorphous materials is attributed to atomic or molecular rearrangement, observed unambiguously in the simulations carried out by Falk and Langer (1998). More recently, Reichhardt et al. (2015) and Lemrich et al. (2017) observe the breaking and making of grain contacts in simulations of a glass bead pack driven by acoustic waves, pointing to the role of STZ rearrangements in controlling the nonlinear behavior. When these rearrangement events involve a spectrum of rates and barriers, it is possible to show that the so-called "multispecies" STZ theory predicts the frequency-dependent viscoelastic response, strain recovery, and stretched-exponential relaxation of density fluctuations in metallic glasses and colloidal materials, above the glass transition temperature (Bouchbinder & Langer, 2011a, 2011b; Langer, 2012). There are structural similarities between colloids and granular materials. Specifically, both classes of materials are composed of disordered "building blocks" which give rise to plasticity when displaced in a nonaffine (i.e., inhomogeneous) and irreversible manner. Thus, it is plausible that the multispecies formulation can be applied to a granular material subject to weak stresses, to understand nonlinear behavior such as softening under stress perturbations and slow recovery upon the cessation of such perturbations. Although other intergranular and intragranular processes such as the action of surface fluid at contact areas, and deformation and dissolution of material at grain contacts (Dieterich & Kilgore, 1994), contribute to aging and healing, the focus of the present work is the role of granular displacement and rearrangement.

We focus on the slow relaxation of the *P* wave modulus, which can be inferred from the recovery of the fundamental resonance frequency in a sample of glass beads. In section 2 we provide a brief overview of the multispecies STZ theory needed for modeling weakly stressed granular media. We specify the distribution of STZ transition barriers in section 3, which will be used to model strain and modulus recovery in section 4, without appealing to deformation and material dissolution at the grain contacts and asperities. We will demonstrate the presence of characteristic recovery time that marks the transition from fast to slow, log linear relaxation. We conclude the paper with a discussion about the need for physics-based constitutive models in earth materials in section 5. We note that the terms "slow dynamics," "aging," and "healing" (e.g., Dieterich & Kilgore, 1994; Nakatani & Scholz, 2004a, 2004b) are used synonymously in this work. The physical model presented in this paper should simplify the incorporation of additional effects of other contributions from cracks, fractures, etc., which we plan to address in the future.

2. Shear-Transformation-Zone Model

As we have alluded to in section 1, shear transformation zones, or STZs, are clusters of grains that are susceptible to nonaffine, irreversible rearrangement that produces plastic strain. The STZ picture is a plausible description of slow relaxation processes in a granular material, during which grains move slowly, changing the local contact configuration and their relative positions at isolated sites, and occasionally moving into a void that opens up in an infrequent manner. Often, grains in an STZ have fewer contacts than average. The availability of free volume is not sufficient for the movement of grains to occur; if grains in an STZ can rearrange themselves under some stress configuration, one easily sees that reversing the deviatoric stress will prevent the rearrangement from occurring altogether. Thus, STZs can be broadly classified into two states, termed "plus" and "minus," corresponding to stable and unstable configurations for irreversible rearrangement in a given deviatoric stress state. When an STZ rearranges and flips from one state to another, thereby changing the local contact topology, it is said to undergo a transition.

Although the term STZ refers explicitly to shear, we emphasize that STZs are the sites where granular rearrangements and local contact changes occur. The stress configuration could be one of shear or, as in the slow relaxation experiments considered in this work, one of uniaxial compression. It could also be an oscillatory stress due to acoustic waves that travel in a well-defined direction and precondition the granular pack. To see that the STZ picture applies even in the case of uniaxial compression, one can compute the deviatoric stress tensor in uniaxial compression and see that the deviatoric stress tensor elements are positive perpendicular to the direction of compression and negative parallel to it. Then a simple coordinate rotation transforms this into a pure shear configuration, one that tends to dilate perpendicular to the direction of compression and compress parallel to it. The two STZ states, plus and minus, correspond to maximum and minimum shear over normal stress due to the applied axial load. Thus, it suffices for us to use the uniaxial stress as the sole stress variable for simplicity. STZs can appear and disappear due to, for example, internal stress fluctuations driven by the motion of surrounding grains, external acoustic vibration, or more generally, processes that create or break contacts and open up voids.

One can readily imagine a broad spectrum of volume barriers for STZ transitions, as well as rates at which STZ transitions can occur. At large prevailing stresses, such as in an earthquake fault during earthquake rupture (e.g., Daub & Carlson, 2008; Lieou et al., 2016) or in the fast-flow regime in laboratory shear cell experiments (e.g., van der Elst et al., 2012), the STZs with low activation barriers will cease to exist before being able to undergo a transition. As such, a single-species description is sufficient for most purposes. This may not be true, however, in a weakly stressed or strained granular material. As we shall see below, the multispecies assumption is needed to explain the slow recovery of the original strength of a granular medium. The theoretical formulation here is largely parallel to (Bouchbinder & Langer, 2011a, 2011b) but adapted to tensile deformation in athermal granular media.

The first step in this formulation is to recognize that the total tensile stress σ acting on the granular material consists of additive contributions of the partial stresses associated with the configurational and kinetic vibrational degrees of freedom, the latter of which is related to the viscoelastic response of the material when strained. Thus,

$$\sigma = \sigma_C + \eta_K * \dot{\epsilon}. \tag{1}$$

Here σ_C is the configurational partial stress that controls granular rearrangement and $\dot{\epsilon}$ is the total strain rate. η_K is the kinetic viscosity and the symbol $*$ denotes a convolution

$$\eta_K * \dot{\epsilon} \equiv \int_{-\infty}^{\infty} \mathrm{d}t' \eta_K(t') \dot{\epsilon}(t - t'). \tag{2}$$

At small stresses, active STZs come in a variety of species with different activation barriers Δ, plausibly of the order of the volume of a single grain. Let the number of STZs in each of the plus and minus states be denoted by $N_{\pm}(\Delta)$. The master equation for STZ transitions is (Bouchbinder & Langer, 2011a, 2011b)

$$\tau \dot{N}_{\pm}(\Delta) = \mathcal{R}(\pm\sigma_C, \Delta) N_{\mp}(\Delta) - \mathcal{R}(\mp\sigma_C, \Delta) N_{\pm}(\Delta) + \rho \left[\frac{N^{\mathrm{eq}}(\Delta)}{2} - N_{\pm}(\Delta) \right]. \tag{3}$$

In equation (3), τ is the inertial time scale. $\mathcal{R}(\pm\sigma_C, \Delta)$ is the rate, in units of τ^{-1}, at which STZ transitions between the two possible states occur; thus, $\mathcal{R}(\pm\sigma_C, \Delta)$ is dimensionless. The terms $\mathcal{R}(\pm\sigma_C, \Delta)N_{\mp}(\Delta) - \mathcal{R}(\mp\sigma_C, \Delta)N_{\pm}(\Delta)$ describe the "flipping" of STZs between the two possible states, which conserves the number of STZs, in compliance with detailed balance. ρ is the intensity of acoustic vibration and other external perturbations, which control the rate at which STZs are created and annihilated and bring the number of STZs to some steady state value N^{eq}. The mechanical noise, traditionally denoted by Γ, is negligible and absent in this formulation, because it is second order in the stress σ_C. Accordingly, the partial plastic strain rate associated with STZs of activation barrier Δ is

$$\dot{\epsilon}^{\mathrm{pl}} = \frac{\epsilon_0}{\tau N}\left[\mathcal{R}(\sigma_C, \Delta)N_-(\Delta) - \mathcal{R}(-\sigma_C, \Delta)N_+(\Delta)\right]. \tag{4}$$

Here ϵ_0 is a dimensionless number of order unity; it sets the size of the plastic strain increment induced by an STZ transition. N denotes the total number of grains in the system. Note that this differs from the expression for the strain rate in a pure shear configuration by a factor of 2; because the system is subject to a pure compressional stress, we have to replace the shear stress s in earlier developments by σ and likewise replace $\dot{\gamma}$ and $\dot{\gamma}^{\mathrm{pl}}$ for the xy and yx components of the strain rate in a shear configuration by $\dot{\epsilon}$ and $\dot{\epsilon}^{\mathrm{pl}}$ and divide by a factor of 2 at the appropriate places (Langer, 2008).

As in the single-species formulation, define the STZ density and orientational bias

$$\Lambda(\Delta) = \frac{N_+(\Delta) + N_-(\Delta)}{N}; \quad m(\Delta) = \frac{N_+(\Delta) - N_-(\Delta)}{N_+(\Delta) + N_-(\Delta)} \tag{5}$$

and the symmetric and antisymmetric combinations of the STZ transition rates

$$\mathcal{C}(\sigma_C, \Delta) = \frac{\mathcal{R}(\sigma_C, \Delta) + \mathcal{R}(-\sigma_C, \Delta)}{2}; \quad \mathcal{T}(\sigma_C, \Delta) = \frac{\mathcal{R}(\sigma_C, \Delta) - \mathcal{R}(-\sigma_C, \Delta)}{\mathcal{R}(\sigma_C, \Delta) + \mathcal{R}(-\sigma_C, \Delta)}. \tag{6}$$

Then, from equation (3), their equations of motion read

$$\tau\dot{\Lambda}(\Delta) = \rho\left[\Lambda^{\mathrm{eq}}(\Delta) - \Lambda(\Delta)\right]; \tag{7}$$

$$\tau\dot{m}(\Delta) = 2\mathcal{C}(\sigma_C, \Delta)\left[\mathcal{T}(\sigma_C, \Delta) - m(\Delta)\right] - \rho\, m(\Delta) - \frac{\tau\dot{\Lambda}(\Delta)}{\Lambda(\Delta)}m(\Delta). \tag{8}$$

The first of these equations says that the STZ density relaxes toward some steady state value Λ^{eq}, while the second equation says that the STZ orientational bias relaxes toward some value controlled by the difference between the forward and backward STZ transition rates. The plastic strain rate becomes

$$\dot{\epsilon}^{\mathrm{pl}} = \frac{2\epsilon_0}{\tau}e^{-1/\chi}\int \mathrm{d}\Delta p(\Delta)\mathcal{C}(\sigma_C, \Delta)\left[\mathcal{T}(\sigma_C, \Delta) - m(\Delta)\right]. \tag{9}$$

This is simply equation (4) integrated over the distribution $p(\Delta)$ of activation barriers. Here we invoked for simplicity the quasi-stationary approximation that $\Lambda(\Delta) \approx \Lambda^{\mathrm{eq}}(\Delta) = 2e^{-1/\chi}$, where χ denotes the compactivity of the granular material. (In an unconsolidated granular material, the compactivity increases with decreasing packing fraction or equivalently increasing porosity; χ is used in favor of either of these quantities because of its direct connection with statistical thermodynamics. See, for example, Lieou and Langer (2012). The second equality sign follows from a lengthy thermodynamic analysis; the quasi-stationary approximation is valid in this case, for Λ evolves on a much faster time scale than the plastic strain rate $\dot{\epsilon}^{\mathrm{pl}}$ itself or the stress. See, for example, Lieou et al. (2015) and Lieou and Langer (2012) for details. In effect we have assumed one single formation volume for all STZs.

The next step is to specify the transition rate $\mathcal{R}(\sigma_C, \Delta)$, which contains essentially all of the interesting dynamics. It is plausible that the transition rate increases with configurational disorder and therefore the compactivity χ (Bouchbinder & Langer, 2011a, 2011b):

$$\mathcal{R}(\sigma_C, \Delta) = R_0(\sigma_C, \Delta)\exp\left[-\frac{\Delta}{\epsilon_Z\chi}\exp\left(-\frac{\epsilon_0\sigma_C}{\sigma\Delta}\right)\right]. \tag{10}$$

This double exponential reflects the intuition that the configurational stress σ_C needed to drive the system over a barrier of height Δ must increase with Δ. As one would expect, $\mathcal{R}(+\sigma_C, \Delta) \ll \mathcal{R}(-\sigma_C, \Delta)$, implying that STZ transitions from the unstable to the stable configuration are heavily favored. Here σ is the pressure and ϵ_Z is the free volume per STZ normalized by the grain volume, inserted here so that the formula for $\mathcal{T}(\sigma_C, \Delta)$ below is consistent with the constraint due to the second law of thermodynamics (see equation (12) below). Then, to linear order in σ_C, we have

$$\mathcal{C}(\sigma_C, \Delta) \approx R_0(0, \Delta)e^{-\Delta/\chi} \tag{11}$$

and

$$\mathcal{T}(\sigma_C, \Delta) \approx \mathcal{T}'(0, \Delta)\sigma_C = \frac{\epsilon_0 \sigma_C}{\epsilon_Z \sigma \chi}. \tag{12}$$

Define the dimensionless quantity (Bouchbinder & Langer, 2011a, 2011b), which corresponds to the STZ transition rate in the weakly stressed limit

$$\nu(\Delta) \equiv 2\mathcal{C}(0, \Delta) = 2R_0(0, \Delta)e^{-\Delta/\chi} \tag{13}$$

and perform a change of variable from Δ to ν; the reason for doing this is that the rates ν but not the barrier heights Δ directly carry information about the dynamics of the system. For example, the probability distribution $\tilde{p}(\nu)$ of ν is

$$\tilde{p}(\nu) = -p(\Delta)\frac{\mathrm{d}\Delta}{\mathrm{d}\nu}. \tag{14}$$

(Note the minus sign because the transition rate ν is expected to decrease with increasing barrier height Δ). Then, to first order in σ_C, equation (9) for the plastic strain rate becomes

$$\dot{\epsilon}^{\mathrm{pl}} = \frac{\epsilon_0}{\tau}e^{-1/\chi}\int \mathrm{d}\nu \tilde{p}(\nu)\nu\left[\frac{\epsilon_0\sigma_C}{\epsilon_Z\sigma\chi} - \tilde{m}(\nu)\right], \tag{15}$$

where $\tilde{m}(\nu) \equiv m(\Delta)$. In addition, the equation of motion for $\tilde{m}$, equation (8), becomes

$$\tau\dot{\tilde{m}} = \frac{\epsilon_0\nu}{\epsilon_Z\sigma\chi}\sigma_C - (\nu + \rho)\tilde{m}(\nu). \tag{16}$$

3. Barrier-Height Distribution

In order for us to perform practical calculations, we need an expression for the barrier-height distribution $p(\Delta)$. At this point let us restrict ourselves to systems that are fully aged or are aging slowly, for which $p(\Delta)$ is determined entirely by the configurational variables, such as the compactivity χ.

Equation (10), as written, implies that Δ is measured downward from some reference volume. As such, it appears that for a wide range of Δ, $p(\Delta)$ ought to be of the form

$$p(\Delta) \propto e^{\Delta/\tilde{\Delta}}, \tag{17}$$

where $\tilde{\Delta}$ is a yet-undetermined parameter. Then, in the limit of small Δ and large transition rate ν, we have $\mathrm{d}\Delta/\mathrm{d}\nu = -\chi/\nu$ from equation (13), so that

$$\tilde{p}(\nu) \propto \nu^{-(1+\zeta)} \tag{18}$$

with $\zeta = \chi/\tilde{\Delta}$. On the other hand, equation (17) cannot be correct in the limit of large Δ and small ν; it must be cut off when $\Delta > \Delta^*$ and $\nu < \nu^*$ for some Δ^* and ν^*. (Because STZ transitions that are slower than the rate at which they are generated and annihilated by vibration do not contribute to the viscoelastic response of the granular material, ν^* may contain information about the external drive amplitude that established the steady state of χ prior to the onset of recovery. For practical purposes, both ν^* and χ will be treated as constant parameters over the course of the recovery process, during which both the strain rate and the stress are small.) As such, in the limit of small ν, we propose that

$$p(\Delta) \propto e^{-\Delta/\tilde{\Delta}_1}, \tag{19}$$

for some grain-scale volume $\tilde{\Delta}_1$, so that

$$\tilde{p}(\nu) \propto \nu^{-(1-\zeta_1)} \tag{20}$$

with $\zeta_1 = \chi/\tilde{\Delta}_1$. To interpolate between the large- and small-ν regimes, we combine equations (18) and (20) and write

$$\tilde{p}(\nu) = \frac{A}{\nu[(\nu/\nu^*)^{\zeta} + (\nu^*/\nu)^{\zeta_1}]}. \tag{21}$$

The normalization constant A ensures that $\int \mathrm{d}\nu\, \tilde{p}(\nu) = 1$.

4. Strain and Modulus Recovery

As seen in experiments (e.g., Johnson & Jia, 2005; Johnson & Sutin, 2005), the aggregate elastic modulus recovers slowly upon the cessation of acoustic perturbation. Modulus recovery can be understood through strain recovery:

$$\sigma = M(t)\epsilon^{\mathrm{el}}(t) = M(t)(\epsilon(t) - \epsilon^{\mathrm{pl}}(t)), \quad t > 0. \tag{22}$$

Here while the granular packing is unsheared, it is subject to a constant pressure σ throughout the recovery process. $M(t)$ is the time-dependent elastic modulus, taken here to be the P wave modulus, and $\epsilon(t)$ is the total strain, being the sum of elastic and plastic contributions. Then, following equation (16), we have, with vibration intensity $\rho = 0$,

$$\tilde{m}(\nu) = \tilde{m}_0 e^{-\nu t/\tau} + \frac{\epsilon_0}{\epsilon_Z \chi}\mathrm{sgn}(\sigma)\left(1 - e^{-\nu t/\tau}\right). \tag{23}$$

As a result, the plastic strain rate is

$$\dot{\epsilon}^{\mathrm{pl}} = \frac{\epsilon_0}{\tau} e^{-1/\chi} \int \mathrm{d}\nu \tilde{p}(\nu)\nu \left(\frac{\epsilon_0}{\epsilon_Z \chi}\mathrm{sgn}(\sigma) - \tilde{m}_0\right) e^{-\nu t/\tau}. \tag{24}$$

This can be integrated with time to yield the plastic strain as a function of time $\epsilon(t)$, subject to the condition that upon the end of the relaxation $\epsilon^{\mathrm{pl}}(t = \infty) = 0$:

$$\epsilon^{\mathrm{pl}}(t) = -\epsilon_0 e^{-1/\chi} \int \mathrm{d}\nu \tilde{p}(\nu) \left(\frac{\epsilon_0}{\epsilon_Z \chi}\mathrm{sgn}(\sigma) - \tilde{m}_0\right) e^{-\nu t/\tau}. \tag{25}$$

In particular, at long enough times t, that is, when $t \ll \tau/\nu^*$, the integral is dominated by small-ν contributions (i.e., $\nu < \nu^*$), so that $\tilde{p}(\nu) \approx (A/\nu)(\nu/\nu^*)^{\zeta_1}$ and

$$\epsilon^{\mathrm{pl}}(t) = -\epsilon_0 e^{-1/\chi} \left(\frac{\epsilon_0}{\epsilon_Z \chi}\mathrm{sgn}(\sigma) - \tilde{m}_0\right) \frac{A(\zeta_1 - 1)!}{(\nu^* t/\tau)^{\zeta_1}}. \tag{26}$$

This can be substituted into equation (22) to calculate the elastic modulus, assuming that the total strain rate $\dot{\epsilon}$ is zero, which implies $\epsilon(t) \equiv \epsilon = \sigma/M_0$, where $M_0 \equiv M(t = \infty)$ is the fully recovered elastic modulus, so that

$$M(t) = \frac{\sigma}{\epsilon(t) - \epsilon^{\mathrm{pl}}(t)} = \frac{\sigma M_0}{\sigma - M_0 \epsilon^{\mathrm{pl}}(t)}. \tag{27}$$

One can easily show that $A = \zeta_1$. In the case $\tilde{m} = 0$, this can be simplified to give

$$\frac{M(t)}{M_0} = \left[1 + \frac{M_0}{\sigma}\mathrm{sgn}(\sigma)\frac{\epsilon_0^2}{\epsilon_Z}\frac{e^{-1/\chi}}{\chi}\frac{\Gamma(\zeta_1 + 1)}{(\nu^* t/\tau)^{\zeta_1}}\right]^{-1}. \tag{28}$$

During the relaxation process, $\sigma < 0$. If $\epsilon_0/(\epsilon_Z \chi)\mathrm{sgn}(\sigma) - \tilde{m}_0 < 0$, then $\epsilon^{\mathrm{pl}}(t) > 0$ and decreases toward zero as $t \to \infty$. As such, the denominator in equation (27) is negative and decreasing in magnitude, so that $M(t)$ is an increasing function of time.

To verify the validity of our theory, we compare our results against the modulus recovery measurements in Johnson and Jia (2005) for a simulated fault gouge composed of glass beads subjected to a fixed confining pressure. In so doing, we unravel some important constraints on the spectrum of barrier heights in an unconsolidated glass bead pack. Figure 1 shows the recovery of the elastic modulus $M(t)$ as a function of time t,

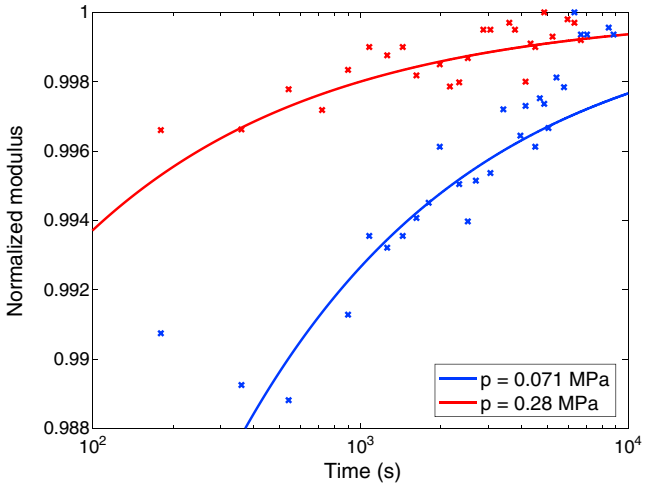

Figure 1. Recovery of the *P* wave modulus of an unconsolidated glass bead pack mimicking fault gouge under a fixed confining pressure, calculated from equations (26) and (27), at two different pressures $\sigma = 0.071$ and 0.28 MPa. The crosses denote the experimentally measured *P* wave modulus, computed from the resonance frequency measurements. See the text for the choice of parameters.

computed from equations (26) and (27). The inertial time scale $\tau = a\sqrt{\rho_G/\sigma}$ is computed using a grain size $a = 0.7$ mm and grain material density $\rho_G = 2.4 \times 10^3$ kg m^{-3}, as in the experiments. In addition, we used $\epsilon_0 = 1.5$, $\epsilon_Z = 0.5$, $\zeta_1 = 0.5$, $\chi = 0.057$, and crucially, $\nu^* = 5 \times 10^{-7}$. The STZ core and void volumes in units of the typical grain size, ϵ_0 and ϵ_Z, should be of order unity; they have been chosen according to convention (e.g., Lieou, Daub, Guyer, et al., 2017; Lieou et al., 2016). The compactivity $\chi = 0.057$ is substantially smaller than the value used to describe shear experiments (typically 0.3) (e.g., Lieou, Daub, Guyer, et al., 2017; Lieou et al., 2016); this reflects the fact that in a densely packed granular medium undergoing relaxation, there are far fewer grain rearrangements than in a sheared granular material. The parameter ν^* is small when there is a large population of "slow" STZs, which delay the recovery of the modulus to the unperturbed value; it can be inferred from a characteristic recovery time that can be extracted from experiment, as discussed later in this manuscript. In addition, we have used $M_0 = 1.31$ GPa for $\sigma = 0.28$ MPa, and $M_0 = 0.872$ GPa for $\sigma = 0.071$ MPa, as inferred from the experiments byJohnson and Jia (2005). We have correctly predicted that the modulus gradually increases as a function of time, and that at a given time t, the modulus increases as a function of the confining stress σ. The exponent ζ_1 has been chosen so that the modulus recovery is approximately logarithmic for the range of times t shown, consistent with the experimental behavior; $\zeta_1 = 0.5$ indicates a broad distribution of barrier heights. For bigger values of the exponent ζ_1, modulus recovery may happen much more rapidly. Thus, the Johnson and Jia (2005) experiments have, in effect, constrained one exponent in the barrier-height distribution.

4.1. Short-Time Behavior

Experiments on Berea sandstone, a consolidated granular material, indicate a characteristic modulus recovery time of about 0.1 s before which the modulus does not increase appreciably as a function of time (Riviere et al. 2016). As far as we know, no experiments have been carried out on glass bead packs to extract the short-time behavior, but we suspect that this might be the case. Note that at short times t the expression for the modulus, equation (28), does not suffice to describe the nonlinear behavior; that expression was derived for the long-time approximation to begin with. Instead, we need the full expression for the STZ distribution $\tilde{p}(\nu)$, equation (21).

From now on, let us suppose that $\zeta = \zeta_1 = 1/2$; the choice of ζ_1 is the same as above, while $\zeta = 1/2$ permits us to proceed analytically and gain important insight below. Then one finds that $A = 1/\pi$, so that equation (21) becomes

$$\tilde{p}(\nu) = \frac{1}{\pi\nu[(\nu/\nu^*)^{1/2} + (\nu^*/\nu)^{1/2}]}. \tag{29}$$

Upon substitution into equation (25), assuming as before that $\tilde{m}_0 = 0$, and using the change of variables $y^2 = \nu/\nu^*$, we find

$$\begin{aligned}\epsilon^{\mathrm{pl}}(t) &= -\frac{\epsilon_0^2 e^{-1/\chi}}{\epsilon_Z \chi}\mathrm{sgn}(\sigma)\int_0^\infty \mathrm{d}y \frac{2e^{-(\nu^* t/\tau)y^2}}{\pi(y^2+1)} \\ &= -\frac{\epsilon_0^2 e^{-1/\chi}}{\epsilon_Z \chi}\mathrm{sgn}(\sigma) e^{\nu^* t/\tau}\mathrm{erfc}\left(\sqrt{\frac{\nu^* t}{\tau}}\right),\end{aligned} \tag{30}$$

where erfc is the complementary error function

$$\mathrm{erfc}(x) = \frac{2}{\sqrt{\pi}}\int_x^\infty e^{-x^2}\mathrm{d}x. \tag{31}$$

Then, equations (28) and (30) together yield

$$\frac{M(t)}{M_0} = \left[1 + \frac{M_0}{\sigma}\mathrm{sgn}(\sigma)\frac{\epsilon_0^2}{\epsilon_Z}\frac{e^{-1/\chi}}{\chi}e^{\nu^* t/\tau}\mathrm{erfc}\left(\sqrt{\frac{\nu^* t}{\tau}}\right)\right]^{-1}. \tag{32}$$

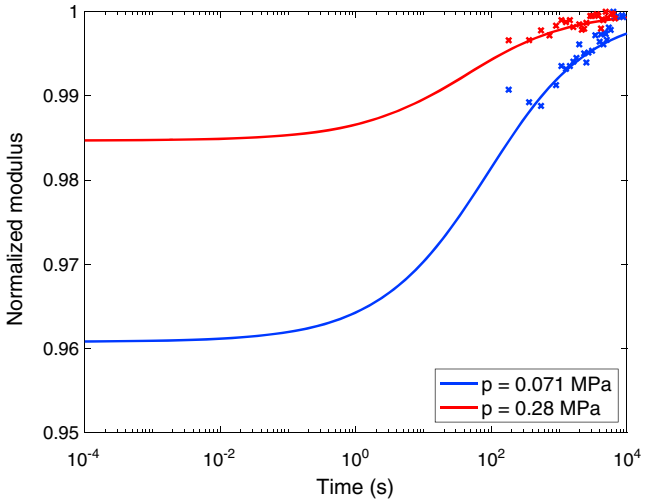

Figure 2. Recovery of the *P* wave modulus, calculated form equations (26) and (27), at two different pressures $\sigma = 0.071$ and 0.28 MPa, for $10^{-4}\text{s} < t < 10^4$ s. The full STZ spectrum, equation (29), has been used. See the text for the choice of parameters.

In particular, in the short-time limit $t \to 0$ we have

$$\frac{M(t \to 0)}{M_0} = \left[1 + \frac{M_0}{\sigma}\text{sgn}(\sigma)\frac{\epsilon_0^2}{\epsilon_Z}\frac{e^{-1/\chi}}{\chi}\right]^{-1}, \tag{33}$$

independent of the parameter ν^* which controls the fraction of slow STZs. Equation (33) may help constrain the compactivity χ given experimental measurements.

Figure 2 shows the modulus recovery as a function of time when the full expression for the STZ probability distribution, equation (29), is employed. Here we have used, as before, $a = 7$ mm, $\rho_G = 2.4 \times 10^3$ kg m^{-3}, $\epsilon_0 = 1.5$, $\epsilon_Z = 0.5$, $\nu^* = 5 \times 10^{-7}$, $M_0 = 1.31$ GPa for $\sigma = 0.28$ MPa, and $M_0 = 0.872$ GPa for $\sigma = 0.071$ MPa. In addition we have chosen $\chi = 0.059$, which differs only slightly from the one used above in the long-time approximation. The long-time behavior is almost identical to that shown in Figure 1 above. Note that while a number of combinations of ν^* and χ can reproduce the long-time limit, their choice has a major implication for the short-time behavior. For example, if one chooses $\chi = 0.073$ and $\nu^* = 5{\times}10^{-4}$, for which there is a small population of slow STZs in a relatively loose glass bead pack, the *P* wave modulus immediately upon the cessation of external vibrations would only be around 65% of its unperturbed value.

4.2. Characteristic Recovery Time and the Different Stages of Aging

In fact, ν^* alone controls the characteristic recovery time, that is, the time t^* at which modulus recovery shows an inflection when time is plotted on a logarithmic scale. This can be seen easily by noting that t appears only in the combination $\nu^* t/\tau$ in the full expression for the modulus, equation (32), so that the characteristic recovery time is

$$t^* = \tau/\nu^*. \tag{34}$$

The dependence of t^* on ν^* can be understood from equation (21), in which ν^* first appeared as a characteristic STZ transition rate in units of the inverse inherent time scale τ^{-1}, or the rate of nonaffine local contact change, that separates the fast STZs with low transition barriers from the slow ones with large barrier heights. Thus, t^* marks the transition from fast recovery at short times, dominated by the motion of fast STZs immediately upon the cessation of external perturbations and corresponding to the rapid breaking and formation of intergrain contacts, to log linear recovery, during which the entire spectrum of STZs participate, in the intermediate time regime. There is a third, long-time regime, when aging is almost complete and the elastic modulus approaches its unperturbed, steady state value; slow STZs dominate this regime, possibly through cooperative motion. In the experiment analyzed here, this corresponds to $t \gtrsim 10^4$ s. We shall term these the early, middle, and late epochs of slow dynamics and aging.

A characteristic recovery time of $t^* \sim 100$ s, which appears to be reasonable, gives $\nu^* \sim \mathcal{O}(10^{-7})$ at the pressures $\sigma = 0.071$ MPa and 0.28 MPa considered in this paper. This confirms that our choice $\nu^* = 5 \times 10^{-7}$ is reasonable. More generally, the characteristic recovery time provides us with an order-of-magnitude estimate for ν^* which, along with knowledge of the long-time behavior, helps constrain χ and provides clues to the short-time behavior which can be tested in experiments for the validity of the theory.

5. Concluding Remarks

In this paper we have developed a mechanistic model for slow relaxation in unconsolidated granular media. The model attributes the recovery of elastic moduli to the slow, configurational dynamics of plasticity carriers known as STZs; these are essentially local clusters of grains susceptible to rearrangement. The STZ picture provides a plausible explanation to the recovery of strain and elastic moduli as STZ transitions are equivalent to changes in local contacts. With rather generic assumptions on the distribution of STZ activation barriers and transition rates, and through constraining a small number of parameters and the initial conditions, we have obtained good agreement with experiments on unconsolidated glass bead packs which mimic a granular fault gouge. Thus, the multispecies STZ theory offers a tenable, physical description of postseismic healing in the first few kilometers of depth on an earthquake fault.

Among the key results of this work, we have shown that the aging process can be divided into three stages: the early regime dominated by the fast hysteretic elements (in this case the STZs); the middle epoch during which the slow STZs prevail, giving rise to log linear recovery in time; and the late epoch when the log linear recovery slows down further and the material transitions into the unperturbed steady state. Equally remarkable is the fact that we have arrived at these results, obtained good fit to experimental measurements, and made predictions for the early time behavior, through the motion of grains and contacts alone, without appealing to deformation and the surface chemistry at the grain contacts. Slow dynamics have indeed been observed in controlled vacuum experiments on Berea sandstone, in which effects of surface chemistry were eliminated (TenCate, 2011). While we do not claim that surface chemistry is irrelevant in the glass bead pack experiments considered in this paper, the fact that slow dynamics can be attributed solely to mechanistic elements is significant. Indeed, if we can explain these observations based on granular motions alone, for a relatively simple glass bead packing where the pressure is comparatively low and surface chemistry is insignificant, this suggests that granular displacement and rearrangement may dominate healing and aging effects in more complex conditions near the Earth surface, whereas other physical processes such as dissolution of materials may be less important.

Physical processes at grain contacts and asperities, however, may have important implications for frictional slip between grains and the rate $\mathcal{R}(\sigma_C, \Delta)$ at which nonaffine rearrangement of grains occurs (e.g., Chen et al., 2015; Karner et al., 1997; Yasuhara et al., 2005). We defer the theoretical modeling of the effects of possible surface chemistry to future work.

Of course, not all geomaterials are unconsolidated or granular in nature; many rock materials, for example, may be polycrystalline. Is it possible to extend our present theoretical approach to encompass polycrystalline rock materials, where the plasticity carriers are dislocations as opposed to STZs? Langer (2015) and Langer et al. (2010) have proposed an effective temperature theory of polycrystalline materials undergoing deformation at large stresses and may provide the first clues to how one may be able to describe dislocation-mediated relaxation in polycrystalline rock materials. It will be interesting to find out whether one can formulate a similar theory for slow relaxation in polycrystalline materials, in analogy to what we have accomplished in this paper.

At this point let us revisit our broader goal and what we have accomplished in the present work. In contrast to phenomenological, empirical theories, and those that attempt to be physics-based, described in section 1 (e.g., Guyer et al., 1995; Lebedev & Ostrovsky, 2014; McCall & Guyer, 1994; Scalerandi et al., 2003; Snieder et al., 2016; Vakhnenko et al., 2004), the STZ approach to nonlinear elasticity of unconsolidated earth materials represents a deeper attempt to provide a solid physical foundation in our theoretical description, to the greatest extent possible. In unconsolidated granular materials, the basic physical process is that of granular displacement and rearrangement and frictional slip between grains. These processes are known to occur at soft clusters of grains, referred to as STZs, whose propensity of occurrence is controlled by the compactivity χ which has its origins in statistical thermodynamics (e.g., Lieou & Langer 2012). Thus, STZ flips described by equation (3), the attribution of plasticity to irreversible granular rearrangement (equation (4)), and the notion of the compactivity are the salient fundamental ingredients of the theory. These do not, however, obviate the need to make empirical assumptions when further physical information is not directly available. Thus, for example, the granular rearrangement rate (equation (10)) and the barrier-height distribution (equations (17) and (19)) are more speculative. When such assumptions are needed, they are made in such a way as to conform with physical intuition, in the simplest and most generic mathematical forms possible. As such, the present work represents not the final step toward an ultimate understanding of complex phenomena in nonlinear elasticity but rather a step forward.

Ben-Naim et al. (1998) proposed an adsorption-desorption model for the slow relaxation and gradual compaction of a granular packing subjected to intermittent "taps" or pulse-like disturbances. Their idea is based on the observation that granular compaction occurs when some void is created due to grain motion and is immediately filled by one of the surrounding grains; this has obvious correspondence to the creation and motion of STZs in our present work. The gradual increase of the packing fraction under successive taps is qualitatively very similar to the gradual recovery of the elastic modulus described in this paper. While the experimental protocols are different, there may be deeper connections between the two sets of phenomena worth exploring.

Slow relaxation and aging is by no means the only class of nonlinear phenomena of interest to the rock physics and seismology communities. The other nonlinear phenomenon is fast nonlinear dynamics—the softening

of the elastic moduli upon increasing the amplitude of dynamic waves beyond some threshold. As an example of the relevance of fast nonlinear dynamics, it has been shown for example by Field et al. (1997) that unconsolidated granular media amplify nonlinear ground motion during an earthquake. We show in a separate paper by Lieou, Daub, Guyer and Johnson (2017) that the STZ theory can describe these phenomena in the time domain prior to that studied in the present manuscript. The possibility of using the STZ theory to describe these phenomena in the time domain prior to that studied in this paper bolsters the applicability of the STZ approach and the utility of physics-based modeling. We believe that theories of this kind, which account for the basic physical processes occurring in a piece of deforming rock material, as opposed to making phenomenological assumptions, represent the future of modeling constitutive behavior in geomaterials. Such theories will help us understand these phenomena observed at scales ranging from laboratory to Earth.

Acknowledgments
We gratefully acknowledge the support of the U.S. DOE Office of Science, Geosciences Division. We also thank Robert Guyer for insightful discussions. C. L. was also partially supported by the Center for Nonlinear Studies at the Los Alamos National Laboratory, with funds from Institutional Support (LDRD). The LANL release number of this article is LA-UR-17-24249. The authors declare no conflict of interest with this work. The data used in this manuscript can be obtained by contacting the corresponding author.

References

Aleshin, V., & Abeele, K. V. D. (2007). Microcontact-based theory for acoustics in microdamaged materials. *Journal of the Mechanics and Physics of Solids*, *55*(2), 366–390. https://doi.org/10.1016/j.jmps.2006.07.002

Ben-Naim, E., Knight, J., Nowak, E., Jaeger, H., & Nagel, S. (1998). Slow relaxation in granular compaction. *Physica D: Nonlinear Phenomena*, *123*(14), 380–385. https://doi.org/10.1016/S0167-2789(98)00136-5, annual International Conference of the Center for Nonlinear Studies.

Bouchbinder, E., & Langer, J. S. (2011a). Linear response theory for hard and soft glassy materials. *Physical Review Letters*, *106*(148), 301. https://doi.org/10.1103/PhysRevLett.106.148301

Bouchbinder, E., & Langer, J. S. (2011b). Shear-transformation-zone theory of linear glassy dynamics. *Physical Review E*, *83*, 61503. https://doi.org/10.1103/PhysRevE.83.061503

Brenguier, F., Campillo, M., Hadziioannou, C., Shapiro, N. M., Nadeau, R. M., & Larose, E. (2008). Postseismic relaxation along the San Andreas Fault at Parkfield from continuous seismological observations. *Science*, *321*(5895), 1478–1481. https://doi.org/10.1126/science.1160943

Brenguier, F., Campillo, M., Takeda, T., Aoki, Y., Shapiro, N. M., Briand, X., … Miyake, H. (2014). Mapping pressurized volcanic fluids from induced crustal seismic velocity drops. *Science*, *345*(6192), 80–82. https://doi.org/10.1126/science.1254073

Chen, J., Verberne, B. A., & Spiers, C. J. (2015). Effects of healing on the seismogenic potential of carbonate fault rocks: Experiments on samples from the Longmenshan Fault, Sichuan, China. *Journal of Geophysical Research: Solid Earth*, *120*, 5479–5506. https://doi.org/10.1002/2015JB012051

Daub, E. G., & Carlson, J. M. (2008). A constitutive model for fault gouge deformation in dynamic rupture simulations. *Journal of Geophysical Research*, *113*, B12309. https://doi.org/10.1029/2007JB005377

Dieterich, J. H., & Kilgore, B. D. (1994). Direct observation of frictional contacts: New insights for state-dependent properties. *Pure and Applied Geophysics*, *143*(1), 283–302. https://doi.org/10.1007/BF00874332

Falk, M. L., & Langer, J. S. (1998). Dynamics of viscoplastic deformation in amorphous solids. *Physical Review E*, *57*, 7192–7205. https://doi.org/10.1103/PhysRevE.57.7192

Falk, M. L., & Langer, J. (2011). Deformation and failure of amorphous, solidlike materials. *Annual Review of Condensed Matter Physics*, *2*(1), 353–373. https://doi.org/10.1146/annurev-conmatphys-062910-140452

Field, E. H., Johnson, P. A., Beresnev, I. A., & Zeng, Y. (1997). Nonlinear ground-motion amplification by sediments during the 1994 Northridge earthquake. *Nature*, *390*, 599–602. https://doi.org/10.1038/37586

Guyer, R. A., & Johnson, P. A. (2009). *Nonlinear mesoscopic elasticity: The complex behavior of granular media including rocks and soil* (2nd ed.), Weinheim, John Wiley.

Guyer, R. A., McCall, K. R., & Boitnott, G. N. (1995). Hysteresis, discrete memory, and nonlinear wave propagation in rock: A new paradigm. *Physical Review Letters*, *74*, 3491–3494. https://doi.org/10.1103/PhysRevLett.74.3491

Jia, X., Brunet, T., & Laurent, J. (2011). Elastic weakening of a dense granular pack by acoustic fluidization: Slipping, compaction, and aging. *Physical Review E*, *84*, 020301. https://doi.org/10.1103/PhysRevE.84.020301

Johnson, P. A., & Jia, X. (2005). Nonlinear dynamics, granular media and dynamic earthquake triggering. *Nature*, *437*, 871–874. https://doi.org/10.1038/nature04015

Johnson, P., & Sutin, A. (2005). Slow dynamics and anomalous nonlinear fast dynamics in diverse solids. *The Journal of the Acoustical Society of America*, *117*(1), 124–130. https://doi.org/10.1121/1.1823351

Karner, S. L., Marone, C., & Evans, B. (1997). Laboratory study of fault healing and lithification in simulated fault gouge under hydrothermal conditions. *Tectonophysics*, *277*(1), 41–55. https://doi.org/10.1016/ S0040-1951(97)00077-2, earthquake Generation Processes: Environmental Aspects and Physical Modelling.

Langer, J. S. (2008). Shear-transformation-zone theory of plastic deformation near the glass transition. *Physical Review E*, *77*, 21502. https://doi.org/10.1103/PhysRevE.77.021502

Langer, J. S. (2012). Shear-transformation-zone theory of viscosity, diffusion, and stretched exponential relaxation in amorphous solids. *Physical Review E*, *85*, 051507. https://doi.org/10.1103/PhysRevE.85.051507

Langer, J. S. (2015). Statistical thermodynamics of strain hardening in polycrystalline solids. *Physical Review E*, *92*, 32125. https://doi.org/10.1103/PhysRevE.92.032125

Langer, J., Bouchbinder, E., & Lookman, T. (2010). Thermodynamic theory of dislocation-mediated plasticity. *Acta Materialia*, *58*(10), 3718–3732. https://doi.org/10.1016/j.actamat.2010.03.009

Lebedev, A. V., & Ostrovsky, L. A. (2014). A unified model of hysteresis and long-time relaxation in heterogeneous materials. *Acoustical Physics*, *60*(5), 555–561. https://doi.org/10.1134/S1063771014050066

Lemrich, L., Johnson, P. A., Guyer, R., Jia, X., & Carmeliet, J. (2017). Dynamic induced softening in frictional granular material investigated by DEM simulation, arXiv. p. arXiv: 1706.05898.

Li, Y.-G., Chen, P., Cochran, E. S., Vidale, J. E., & Burdette, T. (2006). Seismic evidence for rock damage and healing on the San Andreas Fault associated with the 2004 M 6.0 Parkfield earthquake. *Bulletin of the Seismological Society of America*, *96*(4B), S349–S363. https://doi.org/10.1785/0120050803

Lieou, C. K. C., & Langer, J. S. (2012). Non-equilibrium thermodynamics in sheared hard-sphere materials. *Physical Review E*, *85*, 61308. https://doi.org/10.1103/PhysRevE.85.061308

Lieou, C. K. C., Daub, E. G., Guyer, R. A., Ecke, R. E., Marone, C., & Johnson, P. A. (2017). Simulating stick-slip failure in a sheared granular layer using a physics-based constitutive model. *Journal of Geophysical Research: Solid Earth*, *122*, 295–307. https://doi.org/10.1002/2016JB013627

Lieou, C. K. C., Daub, E. G., Guyer, R. A., & Johnson, P. A. (2017). Nonlinear softening of unconsolidated granular earth materials. *Journal of Geophysical Research: Solid Earth*, *122*, 295–307. https://doi.org/10.1002/2017JB014498

Lieou, C. K. C., Elbanna, A. E., & Carlson, J. M. (2016). Dynamic friction in sheared fault gouge: Implications of acoustic vibration on triggering and slow slip. *Journal of Geophysical Research: Solid Earth*, *121*, 1483–1496. https://doi.org/10.1002/2015JB012741

Lieou, C. K. C., Elbanna, A. E., Langer, J. S., & Carlson, J. M. (2014). Shear flow of angular grains: Acoustic effects and nonmonotonic rate dependence of volume. *Physical Review E*, *90*, 32204. https://doi.org/10.1103/PhysRevE.90.032204

Lieou, C. K. C., Elbanna, A. E., Langer, J. S., & Carlson, J. M. (2015). Stick-slip instabilities in sheared granular flow: The role of friction and acoustic vibrations. *Physical Review E*, *92*, 22209. https://doi.org/10.1103/PhysRevE.92.022209

McCall, K. R., & Guyer, R. A. (1994). Equation of state and wave propagation in hysteretic nonlinear elastic materials. *Journal of Geophysical Research*, *99*(B12), 23,887–23,897. https://doi.org/10.1029/94JB01941

Minato, S., Tsuji, T., Ohmi, S., & Matsuoka, T. (2012). Monitoring seismic velocity change caused by the 2011 Tohoku-oki earthquake using ambient noise records. *Geophysical Research Letters*, *39*, L09309. https://doi.org/10.1029/2012GL051405

Nakata, N., & Snieder, R. (2012). Time-lapse change in anisotropy in Japan's near surface after the 2011 Tohoku-oki earthquake. *Geophysical Research Letters*, *39*, L11313. https://doi.org/10.1029/2012GL051979

Nakatani, M., & Scholz, C. H. (2004a). Frictional healing of quartz gouge under hydrothermal conditions: 1. Experimental evidence for solution transfer healing mechanism. *Journal of Geophysical Research*, *109*, B07201. https://doi.org/10.1029/2001JB001522

Nakatani, M., & Scholz, C. H. (2004b). Frictional healing of quartz gouge under hydrothermal conditions: 2. Quantitative interpretation with a physical model. *Journal of Geophysical Research*, *109*, B07202. https://doi.org/10. 1029/2003JB002938

Reichhardt, C. J. O., Lopatina, L. M., Jia, X., & Johnson, P. A. (2015). Softening of stressed granular packings with resonant sound waves. *Physical Review E*, *92*, 22203. https://doi.org/10.1103/PhysRevE.92.022203

Riviere, J., Shokouhi, P., Guyer, R. A., & Johnson, P. A. (2016). Fast and slow nonlinear elastic response of disparate rocks and the influence of moisture. *The Journal of the Acoustical Society of America*, *140*(4), 3326–3326. https://doi.org/10.1121/1.4970596

Rubinstein, J. L., & Beroza, G. C. (2005). Depth constraints on nonlinear strong ground motion from the 2004 Parkfield earthquake. *Geophysical Research Letters*, *32*, L14313. https://doi.org/10.1029/2005GL023189

Scalerandi, M., Delsanto, P. P., & Johnson, P. A. (2003). Stress induced conditioning and thermal relaxation in the simulation of quasi-static compression experiments. *Journal of Physics D: Applied Physics*, *36*(3), 288–293.

Snieder, R., Sens-Schnfelder, C., & Wu, R. (2016). The time dependence of rock healing as a universal relaxation process, a tutorial. *Geophysical Journal International*, *208*, 1–9. https://doi.org/10.1093/gji/ggw377

TenCate, J. A. (2011). Slow dynamics of earth materials: An experimental overview. *Pure and Applied Geophysics*, *168*(12), 2211–2219. https://doi.org/10.1007/s00024-011-0268-4

TenCate, J. A., Smith, E., & Guyer, R. A. (2000). Universal slow dynamics in granular solids. *Physical Review Letters*, *85*, 1020–1023. https://doi.org/10.1103/PhysRevLett.85.1020

Vakhnenko, O. O., Vakhnenko, V. O., Shankland, T. J., & Ten Cate, J. A. (2004). Strain-induced kinetics of intergrain defects as the mechanism of slow dynamics in the nonlinear resonant response of humid sandstone bars. *Physical Review E*, *70*, 15602. https://doi.org/10.1103/PhysRevE.70.015602

van den Wildenberg, S., van Hecke, M., & Jia, X. (2013). Evolution of granular packings by nonlinear acoustic waves. *EPL (Europhysics Letters)*, *101*, 14004.

van der Elst, N. J., Brodsky, E. E., Le Bas, P.-Y., & Johnson, P. A. (2012). Auto-acoustic compaction in steady shear flows: Experimental evidence for suppression of shear dilatancy by internal acoustic vibration. *Journal of Geophysical Research*, *117*, B09314. https://doi.org/10.1029/2011JB008897

Wu, C., Delorey, A., Brenguier, F., Hadziioannou, C., Daub, E. G., & Johnson, P. (2016). Constraining depth range of S wave velocity decrease after large earthquakes near Parkfield, California. *Geophysical Research Letters*, *43*, 6129–6136. https://doi.org/10.1002/2016GL069145

Yasuhara, H., Marone, C., & Elsworth, D. (2005). Fault zone restrengthening and frictional healing: The role of pressure solution. *Journal of Geophysical Research: Solid Earth*, *110*, B06310. https://doi.org/10.1029/2004JB003327